Article

SOURCE DATA | TRANSPARENT PROCESS

THE EMBO JOURNAL

Epigenetic regulation of left–right asymmetry by DNA methylation

Lu Wang[1,2], Zhibin Liu[1,2], Hao Lin[3], Dongyuan Ma[1,2], Qinghua Tao[3] & Feng Liu[1,2,*]

Abstract

DNA methylation is a major epigenetic modification; however, the precise role of DNA methylation in vertebrate development is still not fully understood. Here, we show that DNA methylation is essential for the establishment of the left–right (LR) asymmetric body plan during vertebrate embryogenesis. Perturbation of DNA methylation by depletion of *DNA methyltransferase 1* (*dnmt1*) or *dnmt3bb.1* in zebrafish embryos leads to defects in dorsal forerunner cell (DFC) specification or collective migration, laterality organ malformation, and disruption of LR patterning. Knockdown of *dnmt1* in *Xenopus* embryos also causes similar defects. Mechanistically, loss of *dnmt1* function induces hypomethylation of the *lefty2* gene enhancer and promotes *lefty2* expression, which consequently represses Nodal signaling in zebrafish embryos. We also show that Dnmt3bb.1 regulates collective DFC migration through cadherin 1 (Cdh1). Taken together, our data uncover dynamic DNA methylation as an epigenetic mechanism to control LR determination during early embryogenesis in vertebrates.

Keywords cell adhesion; DNA methylation; dorsal forerunner cells; left–right asymmetry; Nodal signaling

Subject Categories Chromatin, Epigenetics, Genomics & Functional Genomics; Development & Differentiation; Signal Transduction

DOI 10.15252/embj.201796580 | Received 23 January 2017 | Revised 11 August 2017 | Accepted 15 August 2017 | Published online 7 September 2017

The EMBO Journal (2017) 36: 2987–2997

Introduction

DNA methylation is one of the major epigenetic modifications in vertebrates, which involves adding a methyl group to the 5th carbon of cytosine to form 5-methylcytosine (5mC). 5mC is established and maintained by DNA methyltransferases (DNMT), which are classified into two groups, that is, maintenance DNMTs (Dnmt1) and "*de novo*" DNMTs (Dnmt3a and Dnmt3b) (Smith & Meissner, 2013). Genomewide 5mC mapping has implicated the role of DNA methylation during early embryogenesis in that DNMTs maintain the existing DNA methylation pattern to stabilize the genome integrity. In vertebrates, after fertilization, the embryo shows a relatively stable (in zebrafish) or low level (in mice) of DNA methylation before early cleavage stages, and then, the overall DNA methylation level gradually increases until gastrulation (Jiang *et al*, 2013; Potok *et al*, 2013; Wang *et al*, 2014). Various development processes including gastrulation and organogenesis occur after the cleavage stages (Kimelman, 2006). However, our knowledge on how DNA methylation regulates early embryonic development is still limited.

The body pattern determination is initiated during gastrulation, followed by organogenesis. The organs such as the heart, pancreas, liver, and intestines are then asymmetrically positioned within the body cavity. This left–right (LR) asymmetry is first established by symmetry breaking, and then followed by laterality organizer formation, that is, the node in mammals and the Kupffer's vesicle (KV) in zebrafish (Blum *et al*, 2014). The progenitor cells of KV are dorsal forerunner cells (DFCs), which arise from a subset of dorsal surface epithelial (DSE) cells at the sphere stage. The DFC cluster first appears adjacent to the embryonic shield, then migrates to the vegetal pole, and forms a rosette-shaped structure, finally differentiates into ciliated epithelial cells of KV (Oteiza *et al*, 2008). Cilia in laterality organ generate directional fluid flow (i.e., Nodal flow), which thereby leads to asymmetric expression of genes such as Nodal gene (e.g., *spaw* in fish) and its targets (Matsui & Bessho, 2012; Blum *et al*, 2014). This asymmetric expression (usually left side-specific expression of Nodal genes) directs internal organ primordium to position asymmetrically in later stages of development (Okada *et al*, 2005). Several signaling pathways, including Nodal, have been demonstrated to be critical in determining LR asymmetry during vertebrate embryogenesis (Burdine & Schier, 2000; Tanaka *et al*, 2005; Matsui & Bessho, 2012). However, very little is known about the role of epigenetic regulation in LR determination.

In this study, we demonstrate a critical role of DNA methylation in LR asymmetry in vertebrates including zebrafish and *Xenopus*. We show that loss of *dnmt1* or *dnmt3bb.1* disrupts laterality of organs including heart, pancreas, and liver. Mechanistically, hypomethylation of the *lefty2* gene enhancer caused by loss of *dnmt1* can promote *lefty2* expression, which in turn inhibits Nodal signaling, therefore leading to impaired DFC specification and loss of LR asymmetry. In addition, Dnmt3bb.1 is required for *cadherin 1* (*cdh1*)-mediated DFC clustering to ensure proper LR determination.

1 State Key Laboratory of Membrane Biology, Institute of Zoology, Chinese Academy of Sciences, Beijing, China
2 University of Chinese Academy of Science, Beijing, China
3 MOE Key Laboratory of Protein Sciences, Tsinghua University School of Life Sciences, Beijing, China
*Corresponding author. Tel: +86 10 64807307; E-mail: liuf@ioz.ac.cn

Our finding unravels a new layer of regulation involving dynamic DNA methylation in embryonic development in vertebrates.

Results

DNA methylation signal is enriched in the LR organizer

To explore a potential role of DNA methylation in gastrulation, we first knocked down *dnmt1* by injecting *dnmt1* antisense MOs into zebrafish embryos to reduce the global DNA methylation level as reported previously (Rai *et al*, 2006), and then performed MeDIP-seq and RNA-seq in control and *dnmt1*-deficient embryos at early and late gastrulation stages, respectively. The overall methylation level in *dnmt1*-deficient embryos was much lower than that in control embryos (Fig 1A and Appendix Fig S1). Consistently, differential methylation analysis showed that *dnmt1*-deficient embryos had significantly more hypomethylated peaks (n = 1,715) than hypermethylated peaks (n = 284) (Fig 1B). Gene ontology (GO) analysis of genes with differentially methylated peaks in *dnmt1*-deficient embryos revealed an enrichment of genes that are implicated in developmental processes, such as embryo development, pattern specification process, and cell fate commitment (Fig 1C). Notably, genes involved in determination of bilateral symmetry and LR asymmetry were also enriched (Table EV1), indicating a potential role of DNA methylation in this process. Consistently, GO analysis of RNA-seq data showed that developmental process terms were highly enriched among the differentially expressed genes in *dnmt1* morphants, such as determination of bilateral symmetry and pattern specification (Fig EV1A and B). To determine whether DNA methylation is directly involved in LR asymmetry determination, we examined the 5mC level in wild-type embryos using immunofluorescence analysis. 5mC was readily detectable in *sox17*$^+$ DFCs, the progenitor of KV, suggesting potential involvement of DNA methylation in LR determination (Fig 1D). We then investigated which DNMTs are likely to control this process. In zebrafish, there are eight DNMTs, including maintenance DNMT (Dnmt1), "*de novo*" DNMTs (Dnmt3a/b), and Dnmt2 (Campos *et al*, 2012). We examined the expression of *Dnmt* family genes in *sox17*$^+$ DFCs and found that *dnmt1*, *dnmt3bb.2*, *dnmt3bb.1*, and *dnmt3bb.3* were expressed at higher level in DFCs (Fig EV1C). Double fluorescence *in situ* analysis with the DFC marker, *sox17*, further showed that *dnmt1* and *dnmt3bb.1* were specifically enriched in KV and DFCs, respectively (Fig EV1D). Taken together, these data suggest that DNA methylation is possibly involved in LR asymmetry.

DNA methylation is required for LR determination

To investigate whether DNA methylation can modulate LR patterning directly, we injected *dnmt1* MO or *dnmt3bb.1* MO into the yolk at the 512-cell stage as demonstrated previously (Amack & Yost, 2004), to block translation of endogenous *dnmt1* or *dnmt3bb.1* specifically in DFCs. The efficacy of the *dnmt1* translation-blocking MO (atgMO) or *dnmt3bb.1* MO (atgMO) was validated using Western blotting or co-injection with an EGFP plasmid reporter (due to lack of Dnmt3b-specific antibody in zebrafish) (Fig EV2A and Appendix Fig S2). Knockdown of *dnmt1* or *dnmt3bb.1* did not cause any defects during early gastrulation (data not shown). Then, we

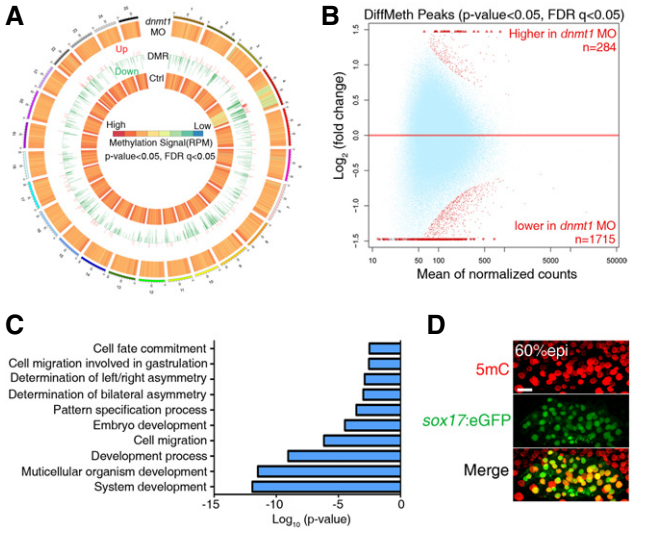

Figure 1. DNA methylation signal is enriched in Left–Right organizer.

A Circos representation of genomewide DNA methylation level in control and *dnmt1* morphants. Each chromosome is marked with different color. The central and outer circles indicate the methylation level in control and *dnmt1*-deficient embryos, respectively. The middle circle displays distribution of DMRs. Decreased and upregulated DMRs in *dnmt1*-deficient embryos are indicated in green and red, respectively. $P < 0.05$, FDR $q < 0.05$.

B Differentially methylated peaks in control and *dnmt1* morphants. $P < 0.05$, FDR $q < 0.05$.

C Gene ontology analysis of genes with DMRs in *dnmt1* morphants.

D Immunofluorescence of 5mC at 60% epi stage in Tg(*sox17*:eGFP) embryos. Scale bar, 20 μm.

examined the knockdown effects on organ laterality. During zebrafish embryogenesis, the initially midline-positioned heart tube undergoes a leftward jogging at 28 h post-fertilization (hpf) (Stainier, 2001). In *dnmt1*-deficient embryos, we observed abnormal cardiac jogging, including rightward and middling looping by detecting *nkx2.5* expression and visualizing heart position in *cmlc2*:GFP transgenic embryos at 30 hpf (Fig 2A). To test the specificity of *dnmt1* MO, we generated *dnmt1* mis-mRNA (with the mutated atgMO target sequence without changing amino acid coding) and co-injected it with *dnmt1* MO into the 1-cell stage embryos. Western blotting results showed that *dnmt1* mis-mRNA can efficiently restore Dnmt1 expression in *dnmt1* morphants (Fig EV2A). As expected, overexpression of *dnmt1* mis-mRNA restored the randomized organ laterality in *dnmt1* morphants (Fig EV2B). Furthermore, a *dnmt1* splice-blocking MO was also used, and its specificity was validated by Western blotting (Fig EV2C). The abnormal cardiac jogging was also found in embryos injected with *dnmt1* splice MO (Fig EV2D), supporting that the disrupted organ laterality was caused by *dnmt1* knockdown specifically. To further confirm these results, we outcrossed the *dnmt1* mutant (*dnmt1*^{s872}) with Tg(*fabp10*:dsRed, *ela3l*:GFP)^{gz12}; Tg(*ins*:dsRed)^{m1081} to examine the organ laterality (Anderson *et al*, 2009). Because of the maternal expression of *dnmt1*, the mutant appeared morphologically normal in comparison with the wild type and heterozygotes (Fig EV2E). Therefore, a low dose of *dnmt1* MO was injected into 1-cell stage embryos including homozygous mutants, wild-type and heterozygous siblings to block

the maternal expression of *dnmt1*. The results showed that a low dose of MO injection failed to affect organ laterality in wild type and heterozygotes, while the injected homozygous mutant exhibited randomized liver and pancreas (Fig EV2E). Collectively, these data support a critical role of *dnmt1* in LR asymmetry.

Interestingly, *dnmt3bb.1* MO^{DFC} embryos also showed abnormal laterality based on examination of the cardiac marker *nkx2.5* at 30 hpf and the liver/pancreas marker, *foxa3* at 46 hpf (Fig 2B), and the modified *dnmt3bb.1* mRNA (*dnmt3bb.1* mis-mRNA) injection can partially restore this abnormal laterality (Fig EV2F). To further confirm these results, we next generated a *dnmt3bb.1* null mutant with an 11-bp insertion in the third exon (236 bp after the start codon) using the CRISPR/Cas9 technique (Fig EV2G). We found that the cardiac jogging was also disturbed in *dnmt3bb.1* mutant (Fig EV2H), indicating an important role of *dnmt3bb.1* in LR development.

Since both *dnmt1* and *dnmt3bb.1* are required for LR patterning, we next investigated whether the LR defects would be more severe in double-knockdown embryos. Examination of *nkx2.5* at 30 hpf indeed revealed more severe abnormal laterality (37 out of 56 embryos) in embryos co-injected with *dnmt1* and *dnmt3bb.1* MOs (Fig 2C), compared to individual morphants (Fig 2A and B).

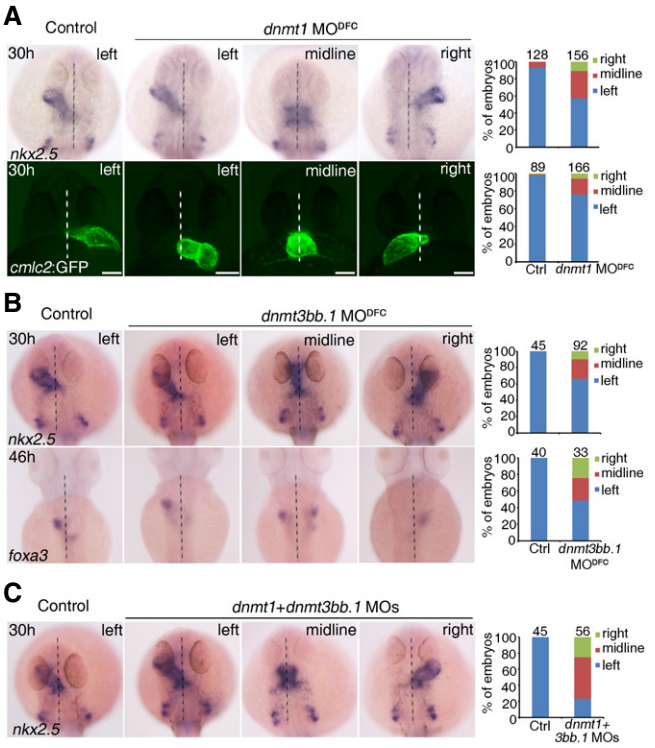

Figure 2. Defects in LR determination in Dnmt morphants.

A–C Representative images showing *nkx2.5* expression in the heart at 30 hpf, *foxa3* expression in visceral organs at 46 hpf or heart looping at 30 hpf using Tg(*cmlc2*: GFP) embryos (bottom panel) in control and DFC-specific-deficient embryos. Statistical analysis is shown on the right with the total observed number of embryos indicated above each bar. Effects of DFC-specific *dnmt1* (A), *dnmt3bb.1* (B), and *dnmt1* + *dnmt3bb.1* (C) knockdown on organ laterality. Scale bar, 100 μm. Dashed lines denote the embryonic midline.

Together, these results demonstrate that DNA methylation is required for organ laterality in zebrafish.

Dnmt1 modulates DFC specification and KV formation

Previous studies in vertebrates including zebrafish, *Xenopus*, chicken and mice have demonstrated that organ laterality is regulated by asymmetric expression of LR genes (Hamada *et al*, 2002; Long *et al*, 2003). We thus analyzed the early asymmetric marker, *southpaw* (*spaw*, the Nodal-related gene in zebrafish), and its downstream target gene *lefty2*. Normally, *spaw* is expressed in the left lateral plate mesoderm (LPM), while *lefty2* is expressed in the anterior LPM at late somitogenesis and later on in the heart primordium on the left side of embryo. Knockdown of *dnmt1* resulted in the randomized expression pattern of *spaw* and *lefty2* (Appendix Fig S3). Given that the asymmetric gene expression is induced by the laterality organizer, we then examined the LR organizer, KV, including organizer formation and ciliogenesis at earlier stages. Live imaging of Tg(*sox17*:eGFP) embryos and immunofluorescence staining using anti-acetylated tubulin showed that *dnmt1* deficiency led to the disrupted lumen formation as well as the decrease in the number and length of primary cilia in the KV (Fig 3A and B). Ciliated epithelial cells of the KV generate the leftward Nodal flow, which is required for LR patterning (Hamada *et al*, 2002). We found that directional KV fluid flow was also disrupted in *dnmt1* morphants (Fig 3C and Movies EV1 and EV2), indicating malformed KV function. Together, these results indicate the requirement of Dnmt1 for KV formation and ciliogenesis.

To investigate whether DNA methylation affects LR patterning through regulation of DFC specification, we examined the expression of early markers specific for DFC fate specification (*sox17*) and differentiation (*foxj1a*), respectively. The expression of these two genes was decreased in *dnmt1* MO^{DFC} embryos and in *dnmt1* splice MO-injected embryos (Figs 3D and EV2I). Furthermore, the number of *sox17*:eGFP-labeled DFCs at shield and 60% epiboly (epi) stages was significantly reduced in *dnmt1* morphants (Fig 3E), indicating that both DFC specification and the cell number were affected by *dnmt1* knockdown. TUNEL assay showed more apoptosis in the DFCs of *dnmt1* morphants, compared to controls, whereas there was no discernable difference on the cell proliferation in DFCs (Appendix Fig S4A and B). In addition, overexpression of *dnmt1* mis-mRNA efficiently rescued the reduced expression of *sox17* and *foxj1a* as well as the number of DFCs at shield stage in *dnmt1* MO-injected embryos (Fig 3F and G). Given there were no obvious differences in the expression of *sox17* in DFCs among embryos from *dnmt1* heterozygous carrier fish, we then used a low dose of *dnmt1* MO injection. As a result, we found a significantly reduced *sox17* expression in homozygous mutant but not in wild-type sibling or heterozygous embryos (Fig EV2J). Collectively, these data suggest that *dnmt1* affects LR asymmetry through modulating DFC specification and KV formation.

Next, to determine whether regulation of LR asymmetry by *dnmt1* is conserved across vertebrates, we used *Xenopus*, a well-established model for LR asymmetry studies (Blum *et al*, 2009). We injected 15–30 ng of *xdnmt1* MO (Dunican *et al*, 2008) into one dorsal blastomere of *Xenopus* embryos at the 4-cell stage and validated its efficiency using Western blotting (Fig EV3A). Examination

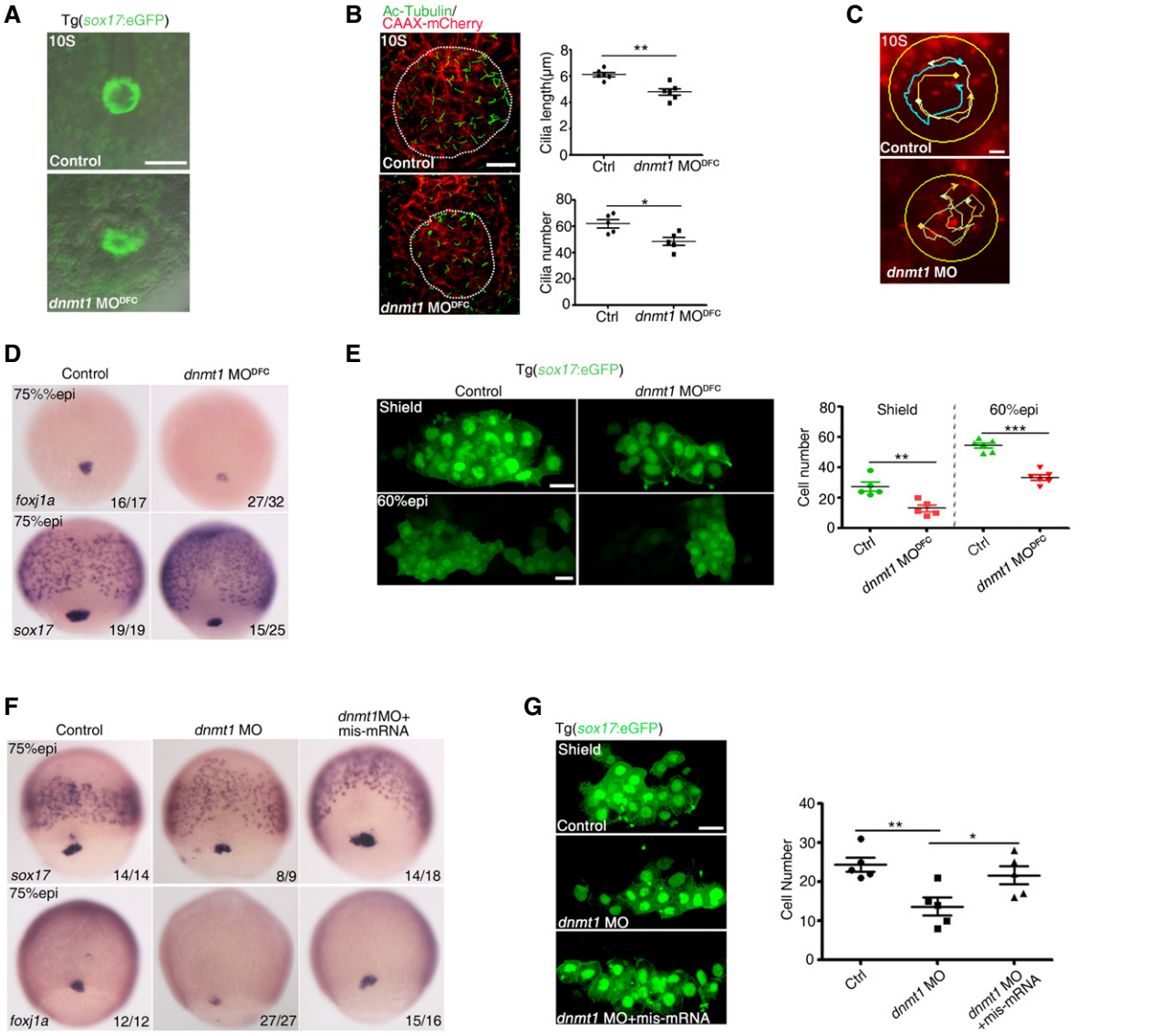

Figure 3. Dnmt1 modulates KV formation and DFC specification.

A Live imaging of KV in Tg(*sox17*:eGFP) embryo. Scale bar, 100 μm.

B Confocal images of cilia immunostained with Ac-tubulin and cell membrane labeled with exogenous CAAX-mCherry in KV region (dashed circles). Right panel shows quantification analysis of cilia number and length. Scale bar, 20 μm.

C KV fluid flow in control embryos and *dnmt1* morphants with bead tracks. Yellow circles denote KV region. Scale bar, 50 μm.

D Expression of *foxj1a* and *sox17* in DFCs in control- and *dnmt1*-deficient embryos.

E DFCs were visualized at shield and 60% epi stage in Tg(*sox17*:eGFP) embryos (left panel). The right panel shows quantification analysis of cell number. Scale bar, 20 μm.

F Injection of *dnmt1* mis-mRNA restored the reduced expression of *sox17* and *foxj1a* in *dnmt1* morphants.

G Visualization of DFCs at 75% epi stage in Tg(*sox17*:eGFP) embryos showing that overexpression of *dnmt1* mis-mRNA restored the number of DFCs in *dnmt1* morphants (left panel) with quantification (right panel). Scale bar, 20 μm.

Data information: (B, E and G) Error bars, mean ± SD, $n \geq 5$ embryos per experiment and $n \geq 2$ technical replicates. *$P <$ 0.05, **$P < 0.01$, ***$P < 0.001$, Student's *t*-test. (D and F) Numbers indicate the number of embryos with the respective phenotype/total number of embryos analyzed in each experiment.

of the heart and gut looping at the tadpole stage showed that about 60% of *xdnmt1* MO-injected embryos (27 out of 47 embryos) exhibited heterotaxia or situs inversus, suggesting a conserved and gene-specific effect of *dnmt1* on the LR patterning in *Xenopus* (Fig EV3B and C). Accordingly, we examined the cilia in gastrocoel roof plate (GRP), the LR organizer of *Xenopus*, by anti-acetylated tubulin staining. The number of acetylated tubulin-positive cilia was decreased on the side that received the *xdnmt1* MO injection, but not on the non-injected side that served as control (Fig EV3D). Collectively, these results demonstrate that DNA methylation is a conserved regulatory mechanism during LR asymmetry determination in vertebrates.

Lefty2 mediates DFC specification downstream of Dnmt1

Our results above reveal an epigenetic regulation of DFC formation by DNA methylation. Numerous studies have demonstrated that the Nodal signaling pathway plays crucial roles in the process of DFC formation, whereas the number of DFCs increases or decreases in response to the enhanced or reduced Nodal signaling, respectively (Schier & Talbot, 2005). As a repressor of Nodal signaling, the elevated *lefty2* expression leads to reduced number of DFCs (Choi *et al*, 2007; Oteiza *et al*, 2008). Since the morphological patterning defects of DFCs observed in *dnmt1*-deficient embryos resemble those of *lefty2*-mRNA-injected embryos (Oteiza *et al*, 2008), we next analyzed *lefty2* expression in *dnmt1*-deficient embryos to test whether *dnmt1* affects DFC formation through altering *lefty2* expression. Whole-mount *in situ* hybridization (WISH) analysis confirmed that the expression of *lefty2* was markedly increased at 60% epi and 75% epi stages in *dnmt1*-deficient embryos (Fig EV4A). Similarly, qPCR analysis also confirmed a significant increase of *lefty2* expression upon *dnmt1* knockdown in manually dissected *sox17*:eGFP^{+} DFCs (Figs 4A and EV4B). Double fluorescence *in situ* hybridization using Tg(*sox17*:eGFP) showed that *lefty2* expression in DFCs was obviously increased upon *dnmt1* deficiency (Fig 4B). We also evaluated the expression of Nodal target genes in DFCs. The qPCR analysis showed that the mRNA levels of these Nodal-regulated genes (*chd*, *ntl*, *dkk1b*, *dusp6*, *gata5*, *id3*, *pitx2a*, and *fgf8*) were decreased in *dnmt1* morphants (Fig 4C). To test whether overexpression of *lefty2* alone can mimic the defects of DFC specification observed in *dnmt1* morphants, we injected *lefty2*-mRNA into *sox17*:eGFP transgenic embryos at 1-cell stage. As expected, overexpression of *lefty2* decreased the number of DFCs in a dose-dependent manner (Fig EV4C).

Next, we tested whether decreasing *lefty2* expression would rescue the LR defects in *dnmt1* morphants. Single *lefty2* MO injection into wild-type embryos did not result in any laterality defects; however, co-injection of *dnmt1* and *lefty2* MOs led to restoration of *sox17* and *foxj1a* expression and the number of DFCs (Figs 4D and EV4D). A significant restoration of Nodal target gene expression was also observed in co-injected embryos (Fig EV4E and F). Moreover, the proportion of embryos with normal heart looping was increased, compared to *dnmt1* morphants and *dnmt1*^{DFC}-injected embryos (Figs 4E and EV4G). Taken together, these results demonstrate that Dnmt1 regulates LR asymmetry through Lefty2-mediated DFC specification.

Dnmt1 represses the expression of *lefty2* through DNA methylation

To verify whether *lefty2* expression alteration in *dnmt1* morphants was directly regulated by DNA methylation. Gene-specific inspection of MeDIP data revealed a region with decreased DNA methylation at the *lefty2* enhancer in *dnmt1*-deficient embryos (Fig 5A). To determine the regulatory potential of this enhancer *in vivo*, we generated an EGFP reporter construct which contains the *lefty2* enhancer and heat-shock protein 70 minimal promoter for a transient expression assay. Consequently, this enhancer construct appeared to fully recapitulate the endogenous *lefty2* expression at gastrulation stage (Fig 5B). Direct sequencing of PCR amplicons from bisulfite-treated DNA of DFCs (Fig EV4B) confirmed the reduced methylation in the *lefty2* enhancer region in *dnmt1*-deficient DFCs (Fig 5C). Importantly, the *lefty2* reporter activity was further increased at 90% epi stage upon *dnmt1* knockdown (Fig 5D). Collectively, these data

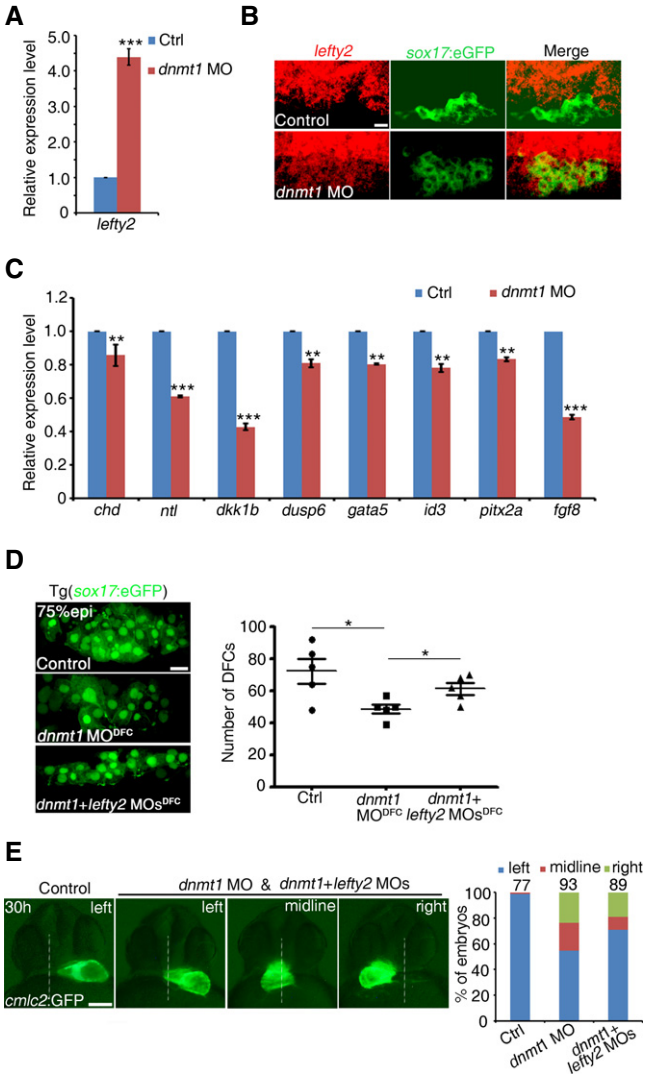

Figure 4. Lefty2 mediates Dnmt1 regulation of DFC specification.

A qPCR analysis of *lefty2* expression in DFCs in control and *dnmt1* MO-injected embryos.

B FISH analysis using Tg(*sox17*:eGFP) showing that *lefty2* expression in DFCs was increased upon *dnmt1* deficiency. Scale bar, 20 μm.

C qPCR analysis of Nodal target genes (*chd*, *ntl*, *dkk1b*, *dusp6*, *gata5*, *id3*, *pitx2a*, *fgf8*) in DFCs.

D Visualization of *sox17*$^{+}$ DFCs in control embryos, *dnmt1* MO^{DFC}- and *dnmt1* + *lefty2* MO^{DFC}-injected embryos (left panel) with quantification (right panel). Scale bar, 20 μm.

E Representative heart looping pattern in Tg(*cmlc2*:GFP) embryos at 30 hpf (left panel) and statistical analysis is shown on the right with the total observed number of embryos indicated above each bar. Scale bar, 100 μm.

Data information: Error bars, mean ± SD, $n = 3$ technical replicates (A and C), $n = 5$ embryos per experiment and $n \geq 2$ technical replicates (D). *$P < 0.05$, **$P < 0.01$, ***$P < 0.001$, Student's *t*-test.

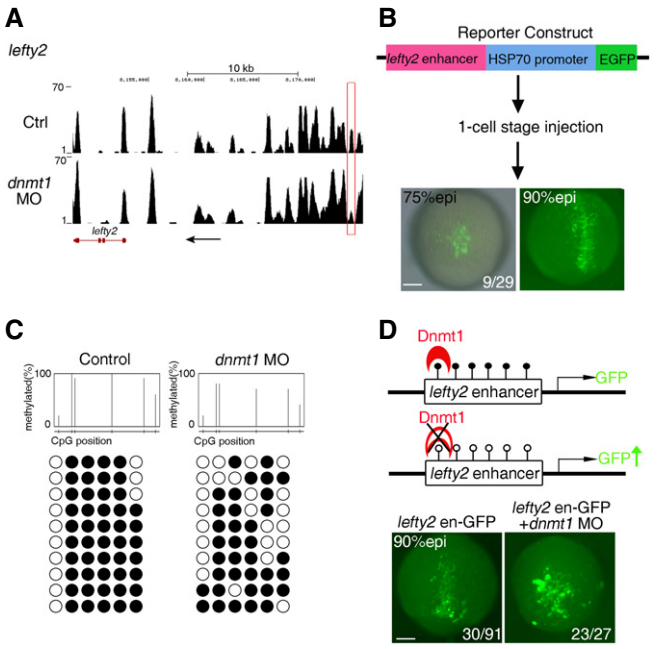

Figure 5. Dnmt1 represses the expression of *lefty2* through DNA methylation.

A MeDIP analysis revealing reduced methylation of an adjacent promoter or distal enhancer of *lefty2*. Red square marks the different region between control and *dnmt1* morphants. The black arrow denotes the transcription direction of *lefty2*.

B Brief diagram of *lefty2* enhancer reporter construct and its activity at gastrulation stages. The number shows the embryos with specific GFP expression in DFC region out of GFP^+ embryos. Scale bar, 100 μm.

C Bisulfite sequencing analysis of DNA methylation at the *lefty2* enhancer (Chr17:8,173,572-Chr17:8,173,845) in DNA isolated from control and *dnmt1* MO-injected DFCs.

D Activity analysis of *lefty2* enhancer indicating increased GFP expression upon *dnmt1* deficiency at 90% epi stage. The numbers show embryos with specific GFP expression in DFC region out of GFP^+ embryos (left panel) or embryos with enhanced GFP out of total embryos with DFC-specific GFP expression (right panel). Scale bar, 100 μm.

demonstrate that *lefty2* is a direct target of Dnmt1 in DFC specification and its upregulation due to enhancer hypomethylation is responsible for the observed DFC and LR defects in *dnmt1*-deficient embryos.

Dnmt3bb.1 regulates collective DFC migration through Cdh1-mediated cell adhesion

Since *dnmt3bb.1* knockdown also caused LR defects, we next sought to explore how *dnmt3bb.1* regulates this process mechanistically. Interestingly, we found that the DFC cluster was less cohesive as manifested by scattered expression patterns of *foxj1a* and *sox17* in *dnmt3bb.1* MO^{DFC} embryos and in *dnmt3bb.1* mutant (Figs 6A and EV5A), but the total number of DFCs appeared to remain unchanged (Fig 6B), which was very different from that observed in *dnmt1*-deficient embryos. Moreover, overexpression of *dnmt3bb.1* mis-mRNA partially restored the disrupted DFC clustering in *dnmt3bb.1* morphants (Fig 6C). These results indicate that DFC clustering is disrupted by *dnmt3bb.1* deficiency. Disaggregation of DFCs suggests a possible involvement of cell adhesion in DFC clustering (Matsui *et al*, 2011, 2015). Previous studies have shown that a tight and stable cluster of DFCs is essential for KV ciliogenesis and LR patterning in zebrafish (Oteiza *et al*, 2010; Matsui *et al*, 2011; Zhang *et al*, 2016). Cdh1-mediated cell adhesion between adjacent DFCs facilitates cell cluster formation, while DFC-specific knockdown of *cdh1* leads to the broken-up DFC phenotype (Matsui *et al*, 2011), similar to what we observed in *dnmt3bb.1*-deficient embryos. qPCR analysis showed that the expression of *cdh1* in the dissected $sox17^+$ DFCs of *dnmt3bb.1*-deficient embryos was significantly decreased (Fig 6D). Phalloidin staining analysis showed altered features of actin filament and local membrane characteristics, upon *dnmt3bb.1* knockdown (Fig 6E). Consistently, *cdh1* knockdown specifically in DFCs also caused defects including disrupted actin filament, disaggregation of DFCs as well as the randomized heart positioning, based on expression patterns of *sox17* and *foxj1a* in DFCs and the *cmlc2*:GFP fluorescence imaging, respectively (Fig 6F and G). Together, these results indicate that Dnmt3bb.1 regulates the cell adhesion of DFCs most likely via *cdh1*. To verify the causal relationship between Dnmt3bb.1 and *cdh1*, we performed rescue experiments using *sox17* and *nkx2.5* as phenotypic readouts. Overexpression of human *cdh1* partially rescued the disrupted DFC clustering and laterality defects in *dnmt3bb.1* morphants (Fig 6H and I). Together, these results demonstrate that Dnmt3bb.1 regulates LR asymmetry through Cdh1-mediated cell adhesion of DFCs.

Our results above indicate that DNA methylation is essential for DFC cluster development. In particular, Dnmt1 regulates the specification of DFCs whereas Dnmt3bb.1 modulates the cohesiveness of DFCs. Examination of DFC cluster in *dnmt1* + *dnmt3bb.1*-deficient embryos showed more severely decreased expression of *sox17* and *foxj1a* and the reduced number of $sox17^+$ cells, indicating that both the cell fate specification and total cell number of DFCs were affected (Fig EV5B and C). To further confirm these results, we used a well-studied DNA methylation inhibitor, 5-aza-2′-deoxycytidine (5-AZA) (Ghoshal *et al*, 2005), to treat embryos from the sphere stage to the shield stage, and then examined the expression of *sox17* and *foxj1a* at shield stage or at 90% epi stage, respectively. 5-AZA-treated embryos showed impaired DFCs (Appendix Fig S5A and B), similar to *dnmt1* + *dnmt3bb.1* double-knockdown embryos (Fig EV5B and C). Additionally, qPCR results showed that the expression of *lefty2* was upregulated, while *cdh1* expression was decreased in 5-AZA-treated embryos (Appendix Fig S5C), consistent with the MO-injection results. Together, these data demonstrate that DNA methylation is required for DFC cluster development.

Discussion

The role of DNA methylation during vertebrate embryogenesis remains largely unclear. Our study demonstrates a critical function of DNA methylation in regulation of LR determination during early embryogenesis in vertebrates. We revealed abnormal organ laterality, DFC and KV malformation when DNA methylation level was attenuated. Mechanistically, Dnmt1 directly acts on the enhancer of *lefty2* to fine-tune the level of Nodal signaling and thus

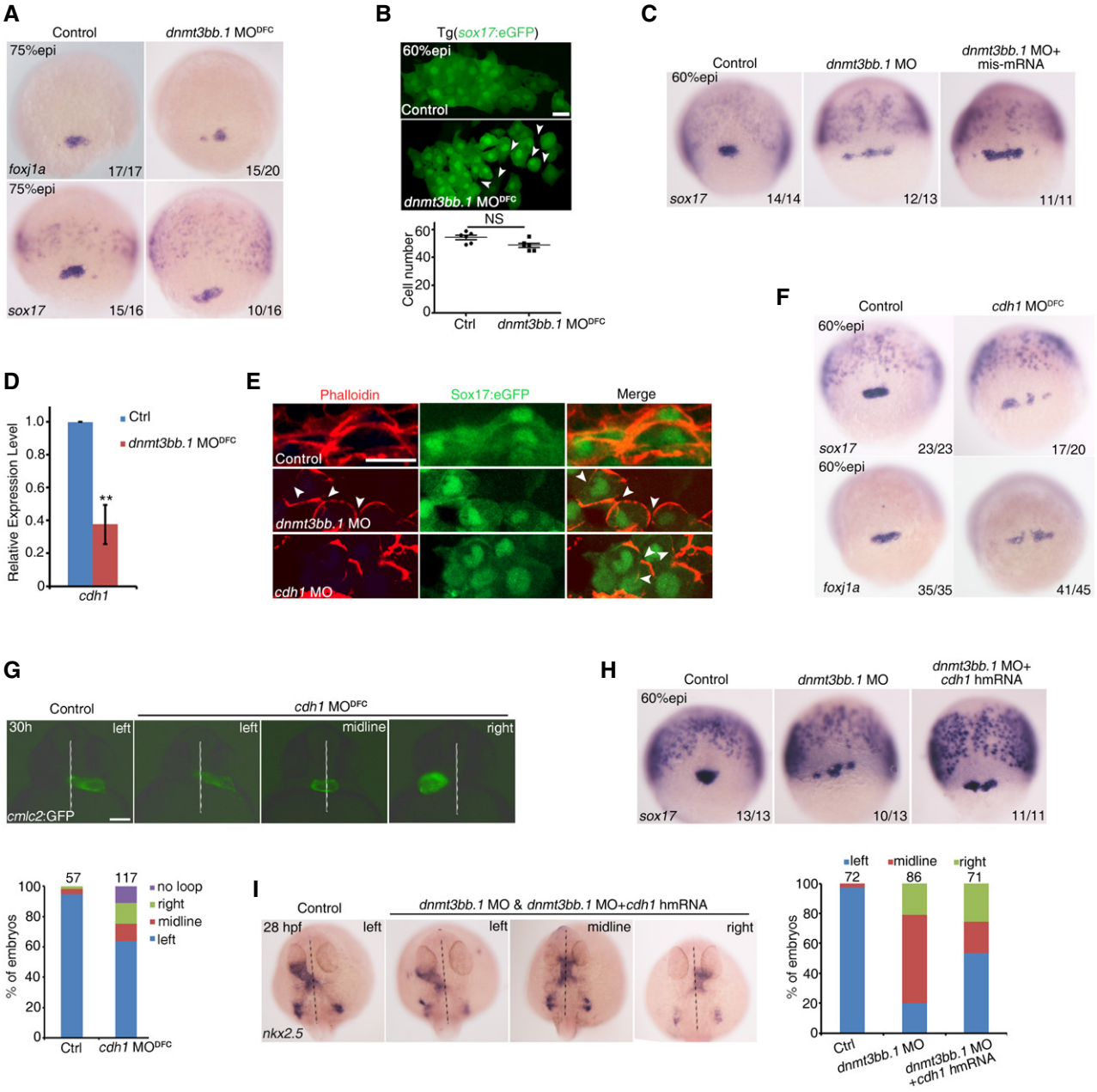

Figure 6. Dnmt3bb.1 regulates DFC clustering through *cdh1*-mediated cell adhesion.

A Expression of *foxj1a* and *sox17* in DFCs in control and *dnmt3bb.1* MO^{DFC}-injected embryos.

B Visualization of *sox17*$^{+}$ DFCs at 60% epi stage in control and *dnmt3bb.1* MO^{DFC}-injected embryos (upper panel) and analysis of cell number (lower panel). Scale bar, 20 μm. The arrowheads denote the disrupted cell-cell contact between DFCs.

C Injection of *dnmt3bb.1* mis-mRNA restored the disrupted *sox17* expression in *dnmt3bb.1* morphants.

D qPCR analysis of *cdh1* expression in DFCs in control and *dnmt3bb.1* MO^{DFC}-injected embryos.

E F-actin of DFCs labeled by phalloidin showing the defects in actin filament and local membrane in *dnmt3bb.1* and *cdh1* morphants, compared with control embryos. Scale bar, 20 μm. The arrowheads denote the disrupted local membrane.

F Reduced expression of *foxj1a* and *sox17* in DFCs at 75% epi stage in *cdh1* MO^{DFC}-injected embryos.

G Representative heart looping pattern in Tg(*cmlc2*:GFP) embryos at 30 hpf. Statistical analysis is shown below with the total observed number of embryos indicated above each bar. Scale bar, 100 μm.

H Human *cdh1* mRNA injection could restore the disrupted *sox17* expression in *dnmt3bb.1* MO-injected embryos.

I Representative heart looping pattern labeled with *nkx2.5* at 28 hpf (left panel). Statistical analysis is shown on the right with the total observed number of embryos indicated above each bar.

Data information: Error bars, mean ± SD, $n = 6$ embryos (B) and $n = 3$ technical replicates (D). $^{**}P < 0.01$, NS, no significance, Student's *t*-test. (C, F and H) Numbers indicate the number of embryos with the respective phenotype/total number of embryos analyzed in each experiment.

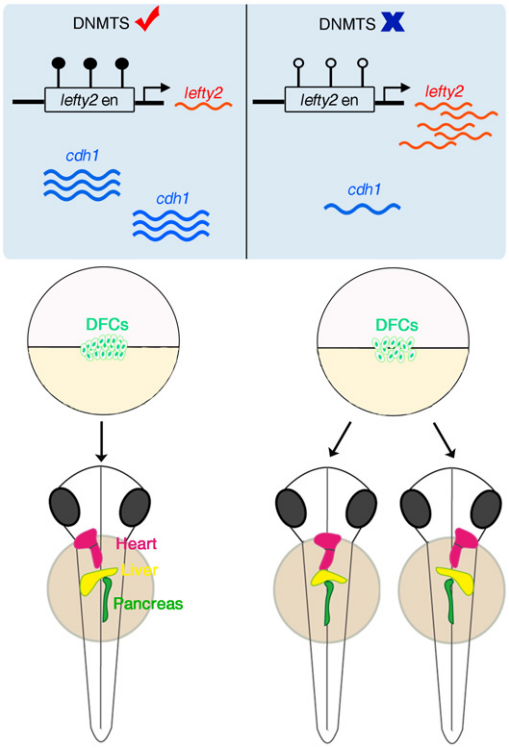

Figure 7. Model for regulation of LR asymmetry by DNA methylation during embryogenesis in vertebrates.

In the presence of DNMTs, the expression of *lefty2* and *cdh1* is tightly controlled to ensure normal LR asymmetry. In the absence of DNMTs, the expression of *lefty2* and *cdh1* is dysregulated due to hypomethylation, thereby causing abnormal LR asymmetry.

modulates DFC specification, while Dnmt3bb.1 is involved in *cdh1*-mediated DFC cohesiveness to ensure LR asymmetry (Fig 7). These findings provide direct evidence for requirements of DNA methylation in the body plan formation during early embryogenesis in vertebrates.

Previous studies have demonstrated the role of DNA methylation during zygotic gene activation after fertilization in vertebrates, including zebrafish, mice, and humans (Jiang *et al*, 2013; Potok *et al*, 2013; Guo *et al*, 2014; Wang *et al*, 2014). The methylation level appears to be stable (in fish) or decreased (in mice) in early cleavage stages of embryos compared to the predicted level in zygote, then increases gradually upon gastrulation (Jiang *et al*, 2013; Potok *et al*, 2013; Wang *et al*, 2014). Early developmental stages including blastula/morula and gastrulation are critical for the body plan determination, such as the formation of three germ layers and establishment of body axis (Tam & Loebel, 2007). Whether DNA methylation is directly involved in these development processes remains unclear. A recent study reported that Tet-mediated DNA demethylation modulates Lefty-Nodal signaling during gastrulation and Dnmt3a/b acts antagonistically to regulate the DNA methylation level of *Lefty* genes in this process (Dai *et al*, 2016). In our work, we reveal that DNA methytransferase1, Dnmt1, directly regulates *lefty2* expression to maintain the balanced Nodal signaling during DFC specification, which is an important pattern specification process during gastrulation, whereas another methyltransferase, Dnmt3bb.1, can target *cdh1*-mediated collective DFC migration at the onset of LR determination. Therefore, our work in zebrafish and the work by Dai *et al* in mice together reveal that dynamic DNA methylation and demethylation are crucial to modulating key signaling pathway during early development from different aspects.

Laterality determination of the vertebrate body plan critically depends on a transient embryonic ciliated organ (Nonaka *et al*, 1998; McGrath *et al*, 2003). Previous studies have demonstrated the evolutionary conservation of laterality organ formation via internalization of DSEs (Kinder *et al*, 2001; Hirokawa *et al*, 2006; Blum *et al*, 2007; Schweickert *et al*, 2007; Oteiza *et al*, 2008). In zebrafish, the ingressed DSEs firstly undergo Nodal signaling-dependent conversion into DFCs, which are the precursors of KV. DFC specification is considered as the initial step of vertebrate laterality organ formation (Oteiza *et al*, 2008). Aberrant development of DFCs would cause reduced KV size, abnormal ciliogenesis, and randomized organ laterality. The molecular mechanisms involved in the specification and formation of DFCs from DSE cells are still poorly understood. Furthermore, DFC clustering and migration are also essential for normal LR asymmetry (Matsui *et al*, 2015), through the cell–cell junction and cell adhesion. Our findings support that DNA methylation mediated by Dnmt1 and Dnmt3bb.1, respectively, modulates the successive steps from the DFC specification, clustering, and migration, to the final organ laterality.

In summary, our studies indicate that DNA methylation-mediated epigenetic modification maintains DFC specification at the onset of gastrulation and determines LR asymmetry, through direct regulation of Nodal signaling. We also show that *cdh1*-mediated cell adhesion during DFC cluster migration is also regulated by DNA methylation as well. Heterotaxia is a group of congenital disorders characterized by a misplacement of one or more internal organs across the LR axis (Peeters & Devriendt, 2006). Given than genetic mechanisms underlying LR asymmetry are well conserved in vertebrates, including humans, a better understanding of regulatory mechanisms of LR asymmetry may contribute to therapies of heterotaxia-related diseases in the clinic.

Materials and Methods

Zebrafish strains and husbandry

Zebrafish strain including AB, Tg(*sox17*:eGFP) (Chung & Stainier, 2008), Tg(*fabp10*:dsRed, *ela3l*:GFP)^{gz12}; Tg(*ins*:dsRed)^{m1081} (Farooq *et al*, 2008), *dnmt1*^{s872} (Anderson *et al*, 2009), and Tg(*cmlc2*:GFP) transgenic lines were raised and maintained at 28.5°C in system water and staged at previously described (Kimmel *et al*, 1995). This study was approved by the Ethical Review Committee of Institute of Zoology, Chinese Academy of Sciences, China.

Xenopus embryos and morpholino

Xenopus eggs and embryos were staged and handled according to standard protocols (Ruzov *et al*, 2004). *xdnmt1* MO (GGACAGGC GTGAAACAGACTCGGC) was injected into blastomere of *Xenopus*

4-cell stage embryos and examined at desired stage (Dunican *et al*, 2008). The GRP was isolated from the embryos at st18 for immunofluorescence of anti-acetylated tubulin. This study was approved by the Ethical Review Committee of Institute of Zoology, Chinese Academy of Sciences, China.

Zebrafish morpholinos and mRNA injection

The following antisense morpholino oligonucleotides (MOs) were used:
dnmt1 MO (ACAATGAGGTCTTGGTAGGCATTTC) (Rai *et al*, 2006);
dnmt1 spliceMO (AGGTCTTGGTAGGCATTTCAAGTTC (This work);
dnmt3bb.1 MO (TTATTTCTTCCTTCCTCATCCTGTC) (Shimoda *et al*, 2005);
lefty2 MO (CAGCTGGATGAACAGAGCCATGCTC) (Feldman *et al*, 2002);
cdh1 MO (TAAATCGCAGCTCTTCCTTCCAACG) (Schotz *et al*, 2008);

1-cell injection and yolk syncytial layer (YSL) injection were performed at 1-cell stage or approximately the 512-cell stage, respectively (Amack & Yost, 2004).

Whole-mount *in situ* hybridization and double fluorescence *in situ* hybridization

Whole-mount *in situ* hybridization with zebrafish embryos was performed as described previously with probes, including *nkx2.5*, *cmlc2*, *foxa3*, *lefty1*, *lefty2*, *southpaw*, *sox17*, *foxj1a*, *ephrinb2b*, *gata6*, and *dnmt1* (Wang *et al*, 2013; Wei *et al*, 2014).

Whole-mount immunofluorescence assay and Western blotting

Whole-mount immunofluorescence was performed as described previously (Wang *et al*, 2013). The following primary antibodies for immunofluorescence were used: anti-5mC (Active Motif, 39649, 1:500), anti-acetylated tubulin (Sigma T6451, 1:500), phosphohistone H3 (Cell Signaling Technology, 9701S, 1:300). Secondary antibodies were Alexa Fluor 488- or 543-conjugated anti-mouse or anti-rabbit IgG. For imaging, the region of DFCs or KV was dissected, embedded in the mounting medium, and was observed using Nikon A1 confocal microscope. Western blotting was performed as previously reported (Wang *et al*, 2013) using anti-Dnmt1 (Santa Cruz Biotechnology, sc-20701, 1:300).

Enhancer construct and reporter assay

The *lefty2* enhancer (Chr17:8,173,572-Chr17:8,173,845) was amplified from zebrafish genomic DNA and linked with the heat-shock protein 70 minimal promoter, then inserted into EGFP reporter vector (pT2AL-EGFP). This construct was injected zebrafish embryos at 1-cell stage and examined at gastrulation stage using fluorescence microscope (Nikon).

Live imaging and KV fluid flow tracking

Tg(*sox17*:eGFP) embryos at a desired stage were manually dechorionated and mounted in 1% low-melting-point agarose. Microscopy was then performed with Nikon or Nikon A1 confocal microscope. To visualize Nodal flow in KV, fluorescent beads of 0.5 μm diameter (Polysciences) were injected into KVs of dechorionated embryos at the 5-somite stage. The embryos at the 10-somite stage were mounted in 1% low-melting-point agarose. The movement of beads was recorded using fluorescence microscope (Leica).

RNA isolation, cDNA synthesis, qPCR

GFP^+ DFCs were dissected from Tg(*sox17*:eGFP) embryos at 75% epi stage using tweezers, and total RNAs were extracted with TRIzol and glycogen, and then, equal amounts of RNA were reversely transcribed and amplified as previously described (Chen *et al*, 2017). The resulting cDNA was used for qPCR using SYBRGreen PCR mixture on a CFX96 Real Time PCR system (Bio-Rad).

Genomic DNA isolation, bisulfite conversion, and sequencing

Appropriate DFCs were directly digested in digestion buffer with proteinase K using EZ DNA Methylation-Direct kit from Zymo research. Then, digested material was bisulfite-converted following manual instructions. Bisulfite-converted DNA was amplified using primers designed by MethPrimer (Li & Dahiya, 2002). Zymo-Taq DNA polymerase enzymes were used for amplifying bisulfite-converted DNA. PCR products were purified and cloned. Mini-prepped colonies were sequenced using T7 sequencing primers. The sequencing results were analyzed using QUMA (Kumaki *et al*, 2008).

Genotyping of *dnmt1*^{s872} mutant

The method for genotyping of *dnmt1*^{s872} was performed as previously described (Anderson *et al*, 2009). A 545-bp DNA fragment spanning the mutation site was amplified from the genomic DNA of *dnmt1*^{s872} embryos by PCR (Forward: 5′-TGGGACGGATTCTTCA GCAC-3′, Reverse: 5′-GCTCCATTTTCTCCTGCTTCACA-3′). 3 μl of the PCR product was digested by HincII at 37°C overnight and fractionated through 2% agarose gel. The uncleaved band represents the wild type without mutation. The DNA fragment from mutants could be cleaved into 360 and 194 bp, while the heterozygous fragment after digestion has three bands (554, 360, and 194 bp).

Generation *dnmt3bb.1* mutant by CRISPR-Cas9

The gRNA target site (GGTGGTGCAGCCTCACCCGC) for *dnmt3bb.1* was designed using the website (http://zifit.partners.org/ZiFiT/), and then synthesized by T7 RNA polymerase and purified using mirVana™ miRNA Isolation Kit (Ambion) *in vitro*. *dnmt3bb.1*-gRNA (70 pg) and Cas9 mRNA (250 pg) were co-injected into one-cell-stage zebrafish embryos. Genomic DNA was extracted from normal developing embryos after injection at 24 hpf. A 465-bp DNA fragment spanning the target site was amplified from the genomic DNA by PCR (P1: 5′-TCAGGCTGC CATGAATCGAG-3′, P2: 5′-TCCCAATGTTGGGTTGTGGC-3′) and sequenced. Founder (F_0) embryos were raised to adulthood and outcrossed with wild-type zebrafish to screen for heritable mutations. Siblings of F_1 embryos carrying mutations were raised to adulthood to establish mutant fish lines.

MeDIP sequencing

Sequencing library was first generated for MeDIP sequencing. The genomic DNA from each sample was sonicated into 200- to 900-base pair (bp) fragments, which were ligated with Illumina genomic adapters using a genomic DNA sample kit (FC-102-1002) according to the user manual. Then, anti-5-methylcytosine antibody was used to precipitate the 300- to 1,000-bp ligated DNA fragments. PCR was performed to amplify the enriched DNA. The quality of the MeDIP and the sequencing library were assessed by quality control (QC). For cluster generation, each sample was diluted to a final concentration of 8 pM, and clusters were generated using an Illumina cBot. Sequencing was performed using an Illumina HiSeq 2000.

RNA sequencing

Total RNA extracted from control and *dnmt1* morphants was reversely transcribed and amplified. cDNA samples were sequenced using Illumina HiSeq 2000 to produce 101-bp paired-end sequence reads. Quality of raw RNA-seq reads for each sample was assessed by quality control (QC) software, and bases with quality scores less than 20 were removed by Trimmomatic. The remaining reads were mapped to the Zebrafish reference cDNA sequences (zv9, from Ensembl) by BWA.

Accession number

The GEO accession number for the MeDIP and RNA-seq data in this study is GSE93927.

Expanded View for this article is available online.

Acknowledgements
We thank Anming Meng, Guo-Liang Xu, and Wei Xie for helpful discussions and critical reading of the paper. This work was supported by grants from the National Natural Science Foundation of China (31425016, 81530004, and 31401242), and the Ministry of Science and Technology of China (2016YFA0100500).

Author contributions
LW performed fish experiments with help from ZL; HL and QT performed *Xenopus* experiments; DM generated the *dnmt3bb.1* mutant; LW and FL conceived the project, analyzed the data, and wrote the manuscript. All authors read and approved the final manuscript.

Conflict of interest
The authors declare that they have no conflict of interest.

References

Amack JD, Yost HJ (2004) The T box transcription factor no tail in ciliated cells controls zebrafish left-right asymmetry. *Curr Biol* 14: 685 – 690

Anderson RM, Bosch JA, Goll MG, Hesselson D, Dong PD, Shin D, Chi NC, Shin CH, Schlegel A, Halpern M, Stainier DY (2009) Loss of Dnmt1 catalytic activity reveals multiple roles for DNA methylation during pancreas development and regeneration. *Dev Biol* 334: 213 – 223

Blum M, Andre P, Muders K, Schweickert A, Fischer A, Bitzer E, Bogusch S, Beyer T, van Straaten HW, Viebahn C (2007) Ciliation and gene expression distinguish between node and posterior notochord in the mammalian embryo. *Differentiation* 75: 133 – 146

Blum M, Beyer T, Weber T, Vick P, Andre P, Bitzer E, Schweickert A (2009) *Xenopus*, an ideal model system to study vertebrate left-right asymmetry. *Dev Dyn* 238: 1215 – 1225

Blum M, Feistel K, Thumberger T, Schweickert A (2014) The evolution and conservation of left-right patterning mechanisms. *Development* 141: 1603 – 1613

Burdine RD, Schier AF (2000) Conserved and divergent mechanisms in left-right axis formation. *Genes Dev* 14: 763 – 776

Campos C, Valente LM, Fernandes JM (2012) Molecular evolution of zebrafish dnmt3 genes and thermal plasticity of their expression during embryonic development. *Gene* 500: 93 – 100

Chen J, Suo S, Tam PP, Han JJ, Peng G, Jing N (2017) Spatial transcriptomic analysis of cryosectioned tissue samples with Geo-seq. *Nat Protoc* 12: 566 – 580

Choi WY, Giraldez AJ, Schier AF (2007) Target protectors reveal dampening and balancing of Nodal agonist and antagonist by miR-430. *Science* 318: 271 – 274

Chung WS, Stainier DY (2008) Intra-endodermal interactions are required for pancreatic beta cell induction. *Dev Cell* 14: 582 – 593

Dai HQ, Wang BA, Yang L, Chen JJ, Zhu GC, Sun ML, Ge H, Wang R, Chapman DL, Tang F, Sun X, Xu GL (2016) TET-mediated DNA demethylation controls gastrulation by regulating Lefty-Nodal signalling. *Nature* 538: 528 – 532

Dunican DS, Ruzov A, Hackett JA, Meehan RR (2008) xDnmt1 regulates transcriptional silencing in pre-MBT *Xenopus* embryos independently of its catalytic function. *Development* 135: 1295 – 1302

Farooq M, Sulochana KN, Pan X, To J, Sheng D, Gong Z, Ge R (2008) Histone deacetylase 3 (hdac3) is specifically required for liver development in zebrafish. *Dev Biol* 317: 336 – 353

Feldman B, Concha ML, Saude L, Parsons MJ, Adams RJ, Wilson SW, Stemple DL (2002) Lefty antagonism of Squint is essential for normal gastrulation. *Curr Biol* 12: 2129 – 2135

Ghoshal K, Datta J, Majumder S, Bai S, Kutay H, Motiwala T, Jacob ST (2005) 5-Aza-deoxycytidine induces selective degradation of DNA methyltransferase 1 by a proteasomal pathway that requires the KEN box, bromo-adjacent homology domain, and nuclear localization signal. *Mol Cell Biol* 25: 4727 – 4741

Guo H, Zhu P, Yan L, Li R, Hu B, Lian Y, Yan J, Ren X, Lin S, Li J, Jin X, Shi X, Liu P, Wang X, Wang W, Wei Y, Li X, Guo F, Wu X, Fan X *et al* (2014) The DNA methylation landscape of human early embryos. *Nature* 511: 606 – 610

Hamada H, Meno C, Watanabe D, Saijoh Y (2002) Establishment of vertebrate left-right asymmetry. *Nat Rev Genet* 3: 103 – 113

Hirokawa N, Tanaka Y, Okada Y, Takeda S (2006) Nodal flow and the generation of left-right asymmetry. *Cell* 125: 33 – 45

Jiang L, Zhang J, Wang JJ, Wang L, Zhang L, Li G, Yang X, Ma X, Sun X, Cai J, Zhang J, Huang X, Yu M, Wang X, Liu F, Wu CI, He C, Zhang B, Ci W, Liu J (2013) Sperm, but not oocyte, DNA methylome is inherited by zebrafish early embryos. *Cell* 153: 773 – 784

Kimelman D (2006) Mesoderm induction: from caps to chips. *Nat Rev Genet* 7: 360 – 372

Kimmel CB, Ballard WW, Kimmel SR, Ullmann B, Schilling TF (1995) Stages of embryonic development of the zebrafish. *Dev Dyn* 203: 253 – 310

Kinder SJ, Tsang TE, Wakamiya M, Sasaki H, Behringer RR, Nagy A, Tam PP (2001) The organizer of the mouse gastrula is composed of a dynamic

population of progenitor cells for the axial mesoderm. *Development* 128: 3623 – 3634

Kumaki Y, Oda M, Okano M (2008) QUMA: quantification tool for methylation analysis. *Nucleic Acids Res* 36: W170 – W175

Li LC, Dahiya R (2002) MethPrimer: designing primers for methylation PCRs. *Bioinformatics* 18: 1427 – 1431

Long S, Ahmad N, Rebagliati M (2003) The zebrafish nodal-related gene southpaw is required for visceral and diencephalic left-right asymmetry. *Development* 130: 2303 – 2316

Matsui T, Thitamadee S, Murata T, Kakinuma H, Nabetani T, Hirabayashi Y, Hirate Y, Okamoto H, Bessho Y (2011) Canopy1, a positive feedback regulator of FGF signaling, controls progenitor cell clustering during Kupffer's vesicle organogenesis. *Proc Natl Acad Sci USA* 108: 9881 – 9886

Matsui T, Bessho Y (2012) Left-right asymmetry in zebrafish. *Cell Mol Life Sci* 69: 3069 – 3077

Matsui T, Ishikawa H, Bessho Y (2015) Cell collectivity regulation within migrating cell cluster during Kupffer's vesicle formation in zebrafish. *Front Cell Dev Biol* 3: 27

McGrath J, Somlo S, Makova S, Tian X, Brueckner M (2003) Two populations of node monocilia initiate left-right asymmetry in the mouse. *Cell* 114: 61 – 73

Nonaka S, Tanaka Y, Okada Y, Takeda S, Harada A, Kanai Y, Kido M, Hirokawa N (1998) Randomization of left-right asymmetry due to loss of nodal cilia generating leftward flow of extraembryonic fluid in mice lacking KIF3B motor protein. *Cell* 95: 829 – 837

Okada Y, Takeda S, Tanaka Y, Izpisua Belmonte JC, Hirokawa N (2005) Mechanism of nodal flow: a conserved symmetry breaking event in left-right axis determination. *Cell* 121: 633 – 644

Oteiza P, Koppen M, Concha ML, Heisenberg CP (2008) Origin and shaping of the laterality organ in zebrafish. *Development* 135: 2807 – 2813

Oteiza P, Koppen M, Krieg M, Pulgar E, Farias C, Melo C, Preibisch S, Muller D, Tada M, Hartel S, Heisenberg CP, Concha ML (2010) Planar cell polarity signalling regulates cell adhesion properties in progenitors of the zebrafish laterality organ. *Development* 137: 3459 – 3468

Peeters H, Devriendt K (2006) Human laterality disorders. *Eur J Med Genet* 49: 349 – 362

Potok ME, Nix DA, Parnell TJ, Cairns BR (2013) Reprogramming the maternal zebrafish genome after fertilization to match the paternal methylation pattern. *Cell* 153: 759 – 772

Rai K, Nadauld LD, Chidester S, Manos EJ, James SR, Karpf AR, Cairns BR, Jones DA (2006) Zebra fish Dnmt1 and Suv39 h1 regulate organ-specific terminal differentiation during development. *Mol Cell Biol* 26: 7077 – 7085

Ruzov A, Dunican DS, Prokhortchouk A, Pennings S, Stancheva I, Prokhortchouk E, Meehan RR (2004) Kaiso is a genome-wide repressor of transcription that is essential for amphibian development. *Development* 131: 6185 – 6194

Schier AF, Talbot WS (2005) Molecular genetics of axis formation in zebrafish. *Annu Rev Genet* 39: 561 – 613

Schotz EM, Burdine RD, Julicher F, Steinberg MS, Heisenberg CP, Foty RA (2008) Quantitative differences in tissue surface tension influence zebrafish germ layer positioning. *HFSP J* 2: 42 – 56

Schweickert A, Weber T, Beyer T, Vick P, Bogusch S, Feistel K, Blum M (2007) Cilia-driven leftward flow determines laterality in *Xenopus*. *Curr Biol* 17: 60 – 66

Shimoda N, Yamakoshi K, Miyake A, Takeda H (2005) Identification of a gene required for de novo DNA methylation of the zebrafish no tail gene. *Dev Dyn* 233: 1509 – 1516

Smith ZD, Meissner A (2013) DNA methylation: roles in mammalian development. *Nat Rev Genet* 14: 204 – 220

Stainier DY (2001) Zebrafish genetics and vertebrate heart formation. *Nat Rev Genet* 2: 39 – 48

Tam PP, Loebel DA (2007) Gene function in mouse embryogenesis: get set for gastrulation. *Nat Rev Genet* 8: 368 – 381

Tanaka Y, Okada Y, Hirokawa N (2005) FGF-induced vesicular release of Sonic hedgehog and retinoic acid in leftward nodal flow is critical for left-right determination. *Nature* 435: 172 – 177

Wang L, Liu T, Xu L, Gao Y, Wei Y, Duan C, Chen GQ, Lin S, Patient R, Zhang B, Hong D, Liu F (2013) Fev regulates hematopoietic stem cell development via ERK signaling. *Blood* 122: 367 – 375

Wang L, Zhang J, Duan J, Gao X, Zhu W, Lu X, Yang L, Zhang J, Li G, Ci W, Li W, Zhou Q, Aluru N, Tang F, He C, Huang X, Liu J (2014) Programming and inheritance of parental DNA methylomes in mammals. *Cell* 157: 979 – 991

Wei Y, Ma D, Gao Y, Zhang C, Wang L, Liu F (2014) Ncor2 is required for hematopoietic stem cell emergence by inhibiting Fos signaling in zebrafish. *Blood* 124: 1578 – 1585

Zhang J, Jiang Z, Liu X, Meng A (2016) Eph/ephrin signaling maintains the boundary of dorsal forerunner cell cluster during morphogenesis of the zebrafish embryonic left-right organizer. *Development* 143: 2603 – 2615